August 27-31, 2023
FLORENCE - ITALY
16th International Conference on Wind Engineering

Wind-Driven Rain technique evaluation for CFD application in an urban area

Payam Gholamalipour[1], Hua Ge and Ted Stathopoulos

BCEE Department, Concordia University, Montreal, Quebec, Canada
[1]Corresponding email: payam.gholamalipour@mail.concordia.ca

SUMMARY:
To design more climate-resilient buildings and to prevent deterioration of historical buildings, Wind-Driven Rain (WDR) loading on facades must be studied. Among the three methods (experimental, CFD, and semi-empirical) of investigating WDR loading on buildings, several sources of errors have been identified using relevant provisions of ISO semi-empirical model for WDR prediction of complex building configurations, such as urban area since the average error can be as high as 218%. The intent of this work is to validate the WDR-CFD models to develop and improve the ISO semi-empirical model, which could then be used for a wide range of building configurations. WDR techniques, i.e., Lagrangian Particle Tracking (LPT) and Eulerian Multiphase (EM) in tandem with realizable $k-\varepsilon$ RANS model have been evaluated in simulating the WDR on a mid-rise building, surrounded by buildings with different dimensions i.e., representing an urban area configuration. Wind and WDR results are compared with the available wind-tunnel (WT) and on-site field measurement (FM) data. The results show higher accuracy and shortened simulation time of the RANS-EM approach over RANS-LPT in the prediction of WDR loading.

Keywords: Wind-driven rain (WDR), Euler-Lagrange vs. Euler-Euler frameworks, Urban area configuration

1. INTRODUCTION

Wind-driven rain (WDR) is one of the main environmental loads, and moisture intrusion from WDR and runoff is a major cause of many building envelope failures. There are two main perspectives for the WDR studies on buildings (Gholamalipour et al., 2022). Firstly, the study of WDR loading on buildings, which is the focus of the current paper, and second, the study of surface response to impinged raindrops. WDR loading on buildings is affected by two major categories of parameters: meteorological and geometrical. Building configuration is found the most influential parameter among geometrical parameters. However, only 13% of previous studies considered WDR loading on geometrically complex configurations in urban area. Furthermore, LPT and EM are both used for modelling the WDR loading coupled with CFD. In the recent past, most researchers have focused on the LPT technique, which is quite challenging to use for parametric analysis and complex circumstances. LPT uses the Euler-Lagrange framework to track thousands of raindrops in a rainfall, which requires a high-resolution computational grid. Both the position and size of the raindrop's injection was usually found by the trial-and-error method so that the raindrops could cover the entire target façade depending on the wind speed, wind direction, and size of the raindrop, the injection plane size and position change. However, a recent study suggests an automated method to select injection plane in a more effective way (Xu et al., 2023). The catch ratio values are calculated by considering the trajectories of raindrops impinging the target façade.

Hence, the pre-processing, solving, and post-processing of the LPT technique results in a high calculation time. In contrast, the EM technique in WDR modelling is based on the Euler-Euler framework, in which raindrops are considered as a continuum phase. Compared to the LPT technique, the EM technique can determine catch ratio values directly from the solved rain phase with lower computational cost, and it does not require an injection plane. The EM technique was shown to be ten times faster than the LPT in terms of simulating the WDR loading on a stand-alone building (Gholamalipour et al., 2022). Therefore, the EM technique has several advantages compared to the LPT technique and it is less challenging to simulate the WDR loading over complex configurations such as an urban area (Gholamalipour et al., 2022).

2. FIELD AND WIND-TUNNEL MEASUREMENTS

The published measurements results of a six-story mid-rise building located in a suburban area in Vancouver, BC, Canada is chosen for the validation. The full-scale dimensions of the test building are 39.7 m long, 15.4 m wide, and 20.1 m high with a mechanical room on top of the roof measuring 5.2 m long, 6.0 m wide, and 2.4 m high. The test building is situated in suburban areas i.e., surrounded by two- to three-story low-rise buildings and trees. Moreover, measurements on a 1:400 scale model of the study building and its surroundings, tested in Concordia University's Atmospheric Boundary Layer (ABL) wind-tunnel, are used to validate the wind flow field (Ge et al., 2017). All surrounding buildings within the 200 m radius of the full-scale test building were considered in the wind-tunnel measurements. Further information on the wind-tunnel and field measurements, and utilized equipment are provided by Chiu (Chiu, 2016).

3. CFD SETTING

OpenFOAM-7 is used to simulate the multiphase flow of wind and WDR in the urban area, developed by (Kubilay et al., 2013). The steady-state realizable k-ε RANS turbulence model is used in tandem with the EM technique. Wind and rain phases are one-way coupled in which the effect of raindrops on the wind flow are neglected, which is a valid assumption as the volumetric ratio of rain phase is kept under 1×10^{-4}. Table 1 summarizes the boundary conditions and parameters used for the wind and rain phases, recommended by (Huang et al., 2012). Moreover, geometry and grid resolution are generated with the Gambit 2.2.2. The computational domain size is generated based on AIJ guidelines for the urban area configuration with dimensions $\text{width} \times \text{depth} \times \text{height} = 793.7 \times 562.2 \times 120.6\ \text{m}^3$ (Tominaga et al., 2008). The blockage ratio is lower than 3%. The distance of upstream, top and lateral boundaries is 5H away from the outer edges of the surroundings of the urban area configuration, in which H=20.1 m is the height of the test building excluding the mechanical room. The downstream boundary is 15H away from the building. Two different grid resolutions with 4 343 782, and 8 248 186 hexahedral cells are executed to determine the grid-sensitivity analysis of the urban area configuration. The fine grid with 8 248 186 cells seems to be sufficient. The distance of the center of adjacent cell to the ground is 0.125 m.

Table 1. CFD boundary conditions of the wind and rain phases for the RANS_EM approach

Boundary	**Wind phase**		**Rain phase**	
Upstream	Velocity inlet	ABL log-law profile	Velocity inlet	$\begin{cases} u_{k,x} = u_x, u_{k,z} = 0, u_{k,y} = -V_t(d) \\ \alpha_k = \frac{R_h f_h(R_h, d)}{V_t(d)} \frac{1 \times 10^{-3}}{3600} \end{cases}$
Top	symmetry	slip walls, adiabatic	Velocity inlet	
Downstream	Outlet	Zero gradient condition	Outlet	$\begin{cases} \frac{\partial \alpha_k}{\partial n} = 0, \frac{\partial \vec{u}_k}{\partial n} = 0 \text{ for } \vec{u}_k.\vec{n} > 0 \\ \alpha_k = 0, \vec{u}_k = 0 \quad \text{for } \vec{u}_k.\vec{n} < 0 \end{cases}$
Ground and buildings	Wall	Standard wall functions	Outlet	
Lateral	Symmetry	slip walls, adiabatic	Symmetry	slip walls, adiabatic

α_k: volume fraction, $f_h(R_h, d)$: raindrop size distribution, R_h: rainfall intensity, $V_t(d)$: terminal velocity d: raindrops diameter size

4. RESULTS AND DISCUSSIONS

4.1. Wind flow

In this study, three different rainfall events are simulated, and the conditions are listed in Table 2. Fig. 1 shows a comparison of normalized mean velocity magnitude, U_{Mag}/U_{ref}, and wind-tunnel measurements and the location of probes. In total there are 49 measurement points located above the mechanical room (wind Monitor) and, on the windward (east) and side (north) facades (Chiu, 2016). Due to the normalization of the mean velocity magnitude with the mean gradient wind speed, U_{ref}, the comparison is valid to all three rainfall events. As shown in Fig. 1b, CFD results are in good agreement with wind-tunnel measurements, particularly for the windward façade, which is our main concern for evaluating WDR. The wind-tunnel validation reveals an average error of 22% on the windward facade (east) and 32% on the side facade (north). Moreover, Fig. 1c shows the normalized mean velocity magnitude, U_{Mag}/U_{ref}, contours and streamlines along horizontal plane (y/H=0.25). The main concern of WDR analysis is the windward façade of the test building, which faces the approaching wind flow. In the urban area configuration, the ground roughness, ABL inflow profiles, and the upstream buildings affect the approaching flow. The flow field upstream of the windward façade of the test building is not symmetrical from the top view, which is greatly altering the catch ratio pattern and values.

Table 2. Overview of various rainfall events condition

Event	U_{10} [m/s]	Direction	u^*_{ABL}[m/s]	y_0 [m]	R_h [mm/hr]	Measurement hours	Date
1	2.41	East	0.232	0.1313	3.16	15	Jan. 2014
2	1.86	East	0.179	0.1313	1.80	2	Sep. 22, 2013
3	2.36	East	0.227	0.1313	1.10	145	Feb. 10-25, 2014

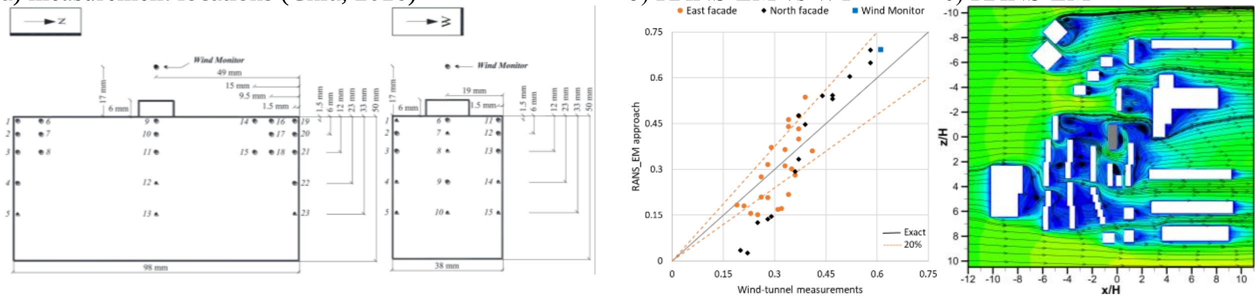
a) measurement locations (Chiu, 2016)
b) RANS-EM vs WT
c) RANS-EM

Figure 1. RANS-EM results comparison of normalized mean velocity magnitude, U_{Mag}/U_{ref}, with available wind-tunnel measurements, and its contour and streamlines along horizontal plane ($y/H = 0.25$) (the test building is highlighted in grey colour)

4.2. Wind-driven rain

Fig. 2 compares the catch ratios and patterns for both WDR techniques, i.e., RANS-LPT and RANS-EM, with the field measurements. The RANS-EM approach is evaluated based on three different rainfall events, listed in Table 2, while RANS-LPT results are available only for rainfall event 2 (Khalilzadeh et al., 2019). Fig. 2b shows that the RANS-EM approach has a better agreement with field measurements than RANS-LPT. The average catch ratio error of 37.5% for the RANS-LPT approach decreases to 31.9% for RANS-EM one (event 2). Fig. 2c-d shows the catch ratio patterns and errors at the WDR gauge locations. As shown in Fig. 1c, the flow field approaching the test building is non-symmetrical so that a non-symmetrical catch ratio pattern is expected on the windward facade as well. The RANS-EM approach appears to be the only one capable of capturing the non-symmetrical patterns.

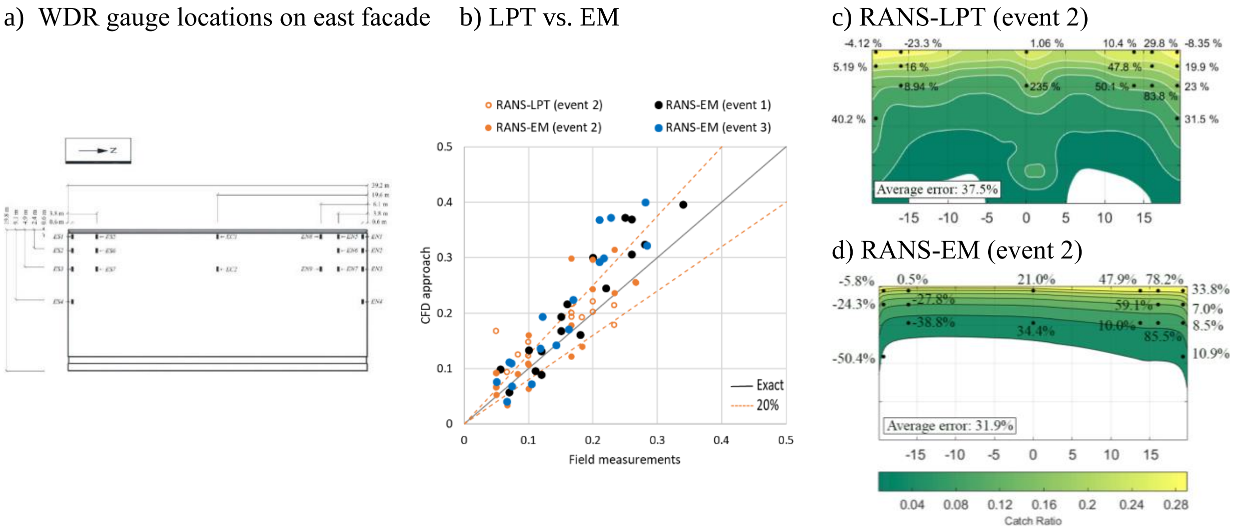

a) WDR gauge locations on east facade b) LPT vs. EM c) RANS-LPT (event 2) d) RANS-EM (event 2)

Figure 2. a) Location of the measurement gauges (Chiu, 2016), b) catch ratio validation of two different WDR techniques based on the field measurements, and c-d) catch ratio pattern comparison

5. CONCLUSIONS

- The RANS-EM wind velocity results against the wind tunnel for the urban area configuration reveals an average error of 22% on the windward facade (east) and 32% on the side facade (north). The windward facade, which is critical for predicting WDR, shows a good agreement.
- WDR analysis of the RANS-EM results demonstrates an improvement over RANS-LPT approach. For the urban area configuration, the average catch ratio error of 37.5% for the RANS-LPT approach decreases to 31.9% for RANS-EM approach (event 2).
- Urban area configuration produces a non-symmetrical catch ratio pattern on the windward facade due to the non-symmetrical approaching flow field upstream of the test building. The non-symmetrical pattern is only captured by the RANS-EM approach. Therefore, RANS-EM is more accurate in predicting WDR values and patterns than RANS-LPT based on the preliminary analysis.

REFERENCES

Chiu, V., 2016. The Effect of Overhang on Wind-Driven Rain Wetting for a Mid-Rise Building. M.Sc. thesis. BCEE Department, Concordia University, Montreal, Canada.

Ge, H., Chiu, V., Stathopoulos, T., 2017. Effect of overhang on wind-driven rain wetting of facades on a mid- rise building : Field measurements. Building and Environment 118, 234–250.

Gholamalipour, P., Ge, H., Stathopoulos, T., 2022. Wind-driven rain (WDR) loading on building facades: A state-of-the-art review. Building and Environment 221, 109314.

Huang, S.H., Ph, D., Li, Q.S., Ph, D., Asce, M., 2012. Large eddy simulations of wind-driven rain on tall building facades. Journal of Structural Engineering 138, 967–983.

Khalilzadeh, A., Hua, G., Dick Ng, H., 2019. Effect of turbulence modeling schemes on wind-driven rain deposition on a mid-rise building: CFD modeling and validation. Journal of Wind Engineering and Industrial Aerodynamics 184, 362–377.

Kubilay, A., Derome, D., Blocken, B., Carmeliet, J., 2013. CFD simulation and validation of wind-driven rain on a building facade with an Eulerian multiphase model. Building and Environment 61, 69–81.

Tominaga, Y., Mochida, A., Yoshie, R., Kataoka, H., Nozu, T., Yoshikawa, M., Shirasawa, T., 2008. AIJ guidelines for practical applications of CFD to pedestrian wind environment around buildings. Journal of Wind Engineering and Industrial Aerodynamics 96, 1749–1761.

Xu, G., Tan, K., Ge, Z., Poh, H.J., Ooi, C.C., Eng, Y., 2023. Automatic selection of release plane for Lagrangian-based wind-driven rain studies. Journal of Wind Engineering and Industrial Aerodynamics 232.